

Hardware-efficient Precise and Flexible Soft-demapping for Multi-Dimensional Complementary APSK Signals

Yoshida, T.; Matsuda, K.; Kojima, K.; Miura, H.; Dohi, K.; Pajovic, M.; Koike-Akino, T.; Millar, D.S.; Parsons, K.; Sugihara, T.

TR2016-121 September 2016

Abstract

We propose the combination of log-likelihood ratio (LLR) table and min-sum algorithm-based LLR updates for simple, precise, and flexible soft-demapping of multi-dimensional complementary APSK signals. Transmission experiment verifies the demapping loss is limited to 0.15 dB in Q-factor.

European Conference on Optical Communication (ECOC)

This work may not be copied or reproduced in whole or in part for any commercial purpose. Permission to copy in whole or in part without payment of fee is granted for nonprofit educational and research purposes provided that all such whole or partial copies include the following: a notice that such copying is by permission of Mitsubishi Electric Research Laboratories, Inc.; an acknowledgment of the authors and individual contributions to the work; and all applicable portions of the copyright notice. Copying, reproduction, or republishing for any other purpose shall require a license with payment of fee to Mitsubishi Electric Research Laboratories, Inc. All rights reserved.

Hardware-efficient Precise and Flexible Soft-demapping for Multi-Dimensional Complementary APSK Signals

Tsuyoshi Yoshida⁽¹⁾, Keisuke Matsuda⁽¹⁾, Keisuke Kojima⁽²⁾, Hiroshi Miura⁽¹⁾, Keisuke Dohi⁽¹⁾, Milutin Pajovic⁽²⁾, Toshiaki Koike-Akino⁽²⁾, David S. Millar⁽²⁾, Kieran Parsons⁽²⁾, and Takashi Sugihara⁽¹⁾

⁽¹⁾ Information Technology R&D Centre, Mitsubishi Electric Corporation, 5-1-1 Ofuna, Kamakura, Kanagawa, 247-8501 Japan, Yoshida.Tsuyoshi@ah.MitsubishiElectric.co.jp

⁽²⁾ Mitsubishi Electric Research Laboratories (MERL), 201 Broadway, Cambridge, MA, 02139, USA.

Abstract We propose the combination of log-likelihood ratio (LLR) table and min-sum algorithm-based LLR updates for simple, precise, and flexible soft-demapping of multi-dimensional complementary APSK signals. Transmission experiment verifies the demapping loss is limited to 0.15 dB in Q-factor.

Introduction

Multi-dimensional (MD) modulations are widely investigated in optical communications^{1,2}. Various MD modulation schemes use block coding over in- and quadrature-phases (I/Q) on two orthogonal polarisations and time slots. Compared to standard modulation formats like regular 2^m -ary quadrature amplitude modulation (QAM), there is a significant improvement in flexibility of spectral efficiency and reach with set-partitioning (SP) by, e.g., single parity check (SPC). Moreover, the coded modulation is useful not only for coding but also for manipulating physical characteristics of the signal³⁻⁵. 4D 2-ary amplitude and 8-ary phase-shift keying (4D-2A8PSK)^{3,4} achieve the same spectral efficiency and better tolerance to fibre nonlinearity compared with dual-polarized (DP) 8QAM family⁶. The 2-ary ASK is complementary between two orthogonal polarisations, and thus 4D-2A8PSK can be generalized to MD complementary APSK (MD-CAPSK) signal, which has constant amplitude of each time slot, Gray mapping, and large Euclidean distance compared to DP-2D modulation schemes.

When such MD modulation is utilized with soft-decision (SD) forward error correction (FEC), soft-demapping is required to generate the input signal of the SD-FEC decoder. Although there are a few reports for 4D-QAM⁷ and 2D-APSK⁸ in optical communications, the technique for 4D or higher-dimensional APSK has not been well investigated so far.

In this paper, we propose an efficient soft-demapping technique, which utilizes 2D log-likelihood ratio (LLR) tables and min-sum algorithm-based LLR updates. This is applicable to MD-CAPSK signals flexibly. We examined the technique in 4D-2A8PSK through nonlinear experiment with offline processing. It is shown that the performance degradation of the proposed soft-demapping is limited to 0.15 dB based on analysis with generalized mutual information (GMI)⁹. The overall performance

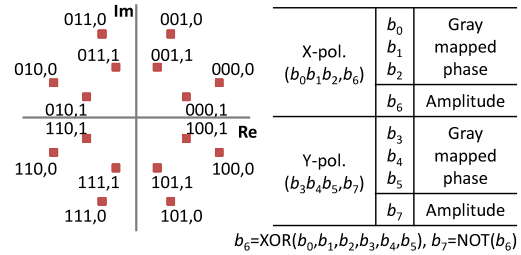


Fig. 1: Bit-to-symbol mapping of MD-CAPSK (an example of 6 bit/symbol 4D-2A8PSK).

improvement of 4D-2A8PSK reaches 0.5 dB against DP-Star-8QAM.

Multi-dimensional CAPSK

Figure 1 shows the mapping rule of 6 bit/symbol 4D-2A8PSK, which is an example of MD-CAPSK signals. ASK is complementary over polarisations, and PSK is Gray mapped. Set-partitioning can be applicable. In the case of 4D-2A8PSK³, the bit b_6 is a parity of SPC code generated by exclusive OR (XOR) of all of the modulation bits; b_0 to b_5 . The other parity bit b_7 is the invert of b_6 . The amplitudes of X and Y polarisations are modulated by b_6 and b_7 , respectively. The power of each 4D symbol is constant due to the complementary ASK in the two polarisations. The optimum ring ratio, defined as the inner ring radius divided by the outer one, is 0.6 to 0.65 for 4D-2A8PSK.

The proposed soft-demapping technique

Figure 2 shows a functional block diagram of the proposed soft-demapping circuit for 4D-2A8PSK, which consists of three blocks.

The first function is 2D LLR tables in X and Y polarisations. Each table inputs are I/Q levels and the corresponding outputs are $\beta_i^{(0)}$ which are LLRs of b_i , including parities of MD coding. The input amplitude levels and the output bit-LLRs have finite resolution. As for 4D-2A8PSK, bit-LLRs in X(Y)-polarisation are derived from a table having input address of XI and XQ (YI and YQ) levels and output of LLRs of 4-bit tributaries $\beta_0^{(0)}, \beta_1^{(0)}, \beta_2^{(0)}, \beta_6^{(0)}$ ($\beta_3^{(0)}, \beta_4^{(0)}, \beta_5^{(0)}, \beta_7^{(0)}$). Examples

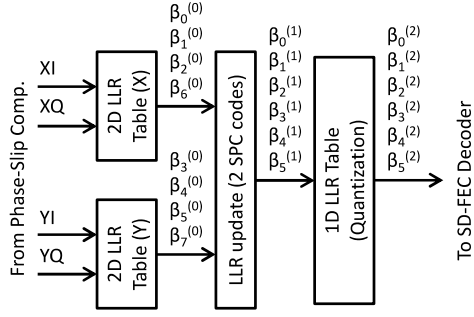


Fig. 2: Soft-demapping circuit for 4D-2A8PSK.

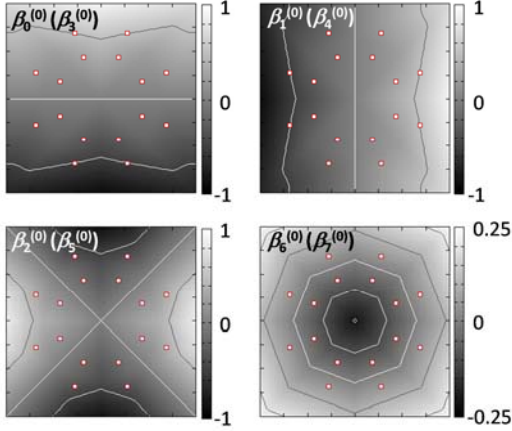


Fig. 3: Contour map example of normalized bit-LLRs $\beta_i^{(0)}$ as a function of input (I,Q) levels in 2D LLR table.

of output bit-LLRs (normalized) as a function of input (I,Q) levels in 2D LLR table is shown in Fig. 3. We assume the signal as 2A8PSK in each polarisation and store four bit-LLRs corresponding to (I,Q) levels precisely.

The second function is LLR update. The bit-LLRs $\beta_0^{(0)}$ to $\beta_7^{(0)}$ are updated by min-sum algorithm⁷ based on the SPC coding related to parities of b_6 and b_7 . By employing the following equations (1) and (2), the extrinsic information $\alpha_{i,j}$ for bit i related to parity bit b_j ($j \in \{6,7\}$) is calculated. SPC code for b_6 is XOR of b_0 to b_6 is zero and that for b_7 is XOR of b_0 to b_5 , and b_7 is one, so the considered bit-sets are $s(6) \in \{0,1,2,3,4,5,6\}$ and $s(7) \in \{0,1,2,3,4,5,7\}$.

$$\alpha_{i,6} = \prod_{k=s(6), k \neq i} \text{sgn}(\beta_k^{(0)}) \min_{k=s(6), k \neq i} |\gamma_k \beta_k^{(0)}| \quad (1)$$

$$\alpha_{i,7} = - \prod_{k=s(7), k \neq i} \text{sgn}(\beta_k^{(0)}) \min_{k=s(7), k \neq i} |\gamma_k \beta_k^{(0)}| \quad (2)$$

As shown in equation (3), the bit-LLR $\beta_i^{(0)}$ is added with the sum of the extrinsic information with the weight ε .

$$\beta_i^{(1)} = \beta_i^{(0)} + \varepsilon(\alpha_{i,6} + \alpha_{i,7}) \quad (3)$$

According to the signal distribution¹⁰, different weighting on $\beta_6^{(0)}$ and $\beta_7^{(0)}$ by γ_k ($k = 6,7$) were applied during the min-sum update. Only one update was sufficient, and the second update did not have a major impact. We

optimized the weight of extrinsic information as $\varepsilon = 0.5$.

The third function is LLR quantization. The updated bit-LLRs except for MD coding parities, $\beta_0^{(1)}$ to $\beta_5^{(1)}$ for 4D-2A8PSK, are quantized by 1D LLR tables to fit the resolution with the SD-FEC decoder input interface. The final bit-LLRs are derived as $\beta_0^{(2)}$ to $\beta_5^{(2)}$.

We choose the number of quantization levels as 64 at both input and output of 2D LLR tables for the first function, 64 and 16 at the input and output of the 1D LLR table for the third function. If 4D LLR tables with 64 levels input are used instead of the proposed technique, the table address becomes unrealistic high at 64^4 (1677216). This 2D LLR table technique can drastically save the address count to 64^2 (4096) with minor performance degradation.

By implementing the first function of 2D LLR table as rewritable and the second function of LLR update as being applicable to flexible SPC coding, the proposed soft-demapping circuit can easily be extended to the other MD-CAPSK-based formats.

Experimental validation

We have conducted transmission experiment by using the setup shown in Fig. 4. The modulation format was 4D-2A8PSK or DP-Star-8QAM. The ring ratio for 4D-2A8PSK was set to 0.6. The baud rate was 32 Gbaud and the roll-off factor of root-raised-cosine filtering at transmitter equalizer (EQ) was 0.15. The digital-to-analogue converter was operated at 64 GS/s. The WDM signal was generated with a bulk modulation of 70 continuous waves spaced at 50 GHz, and which were then de-correlated via 4 signal paths having different delays. The transmission line was 1,260 km, having an average span length of

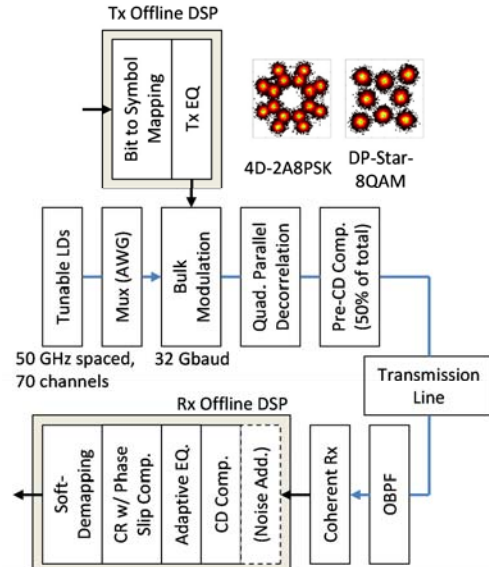


Fig. 4: Experimental setup.

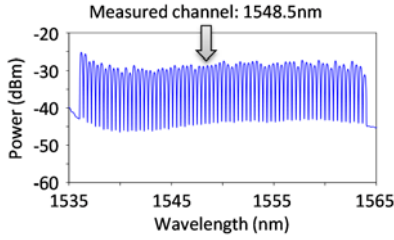


Fig. 5: Received optical spectrum.

70 km, and repeater noise figure (NF) of close to 5 dB. Chromatic dispersion (CD) was managed in-line by the mixture of non-zero dispersion shifted fibre (NZDSF) having negative local CD of -3 ps/nm and standard single-mode fibre (SSMF). The default received optical signal-to-noise ratio (OSNR) was 19.9 dB in 0.1 nm resolution at -2.9 dBm/ch launched power. Figure 5 shows a received optical spectrum of whole WDM signals. One half of the total accumulated CD was compensated at the transmitter. The received signal was coherently detected after wavelength demultiplexing via an optical bandpass filter (OBPF). Each laser linewidth including local oscillator was < 500 kHz and the measured wavelength was 1548.5 nm. The signal stored by 64 GS/s analogue-to-digital converters (ADCs) was processed offline, which included CD compensation, adaptive equalization with constant modulus algorithm for initial convergence and radius directed equalization afterward, carrier recovery (CR) with multi-pilot algorithm¹¹ having a window size of 63, pilot-aided phase-slip recovery, and the proposed soft-demapping. Note that, for DP-Star-8QAM, we also used a 2D LLR table in each polarisation, whose input is 64 levels per dimension and 16 levels output per bit.

The performance was evaluated by not hard-decision bit-error rate (BER)-based Q-factor; $Q_{BER}^2 = 2 \cdot \{\text{erfc}^{-1}(2 \cdot BER)\}^2$ but by GMI-based one; $Q_{GMI}^2 = \{0.5 \cdot J^{-1}(GMI)\}^2$, where inverse J function is well known in extrinsic information transfer chart analysis¹². The defined Q-factor from GMI (or BER) means an SNR to obtain the corresponding GMI (BER) in binary-input additive white Gaussian noise channels.

Figure 6 shows the experimental results; Fig. 6 (a) is Q from GMI as a function of launched power. In the case of ideal soft-demapping (only 16 level quantization for SD-FEC decoding was applied), we observed 0.6 dB improvement at maximum Q by 4D-2A8PSK compared to DP-Star-8QAM. The proposed technique had performance degradation of 0.15 dB and 0.06 dB for 4D-2A8PSK and DP-Star-8QAM, respectively. The overall performance gain of 0.5 dB was still significant in the highly nonlinear

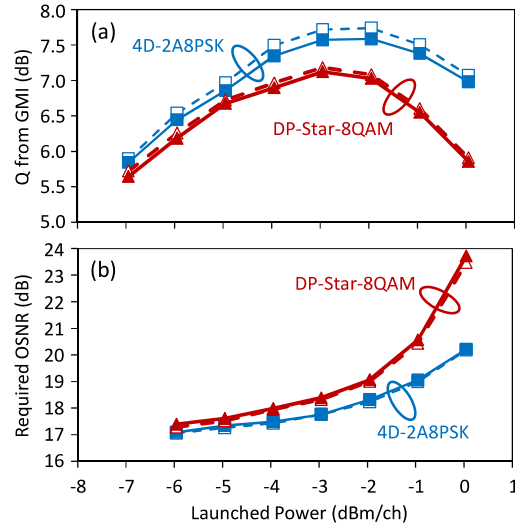


Fig. 6: Experimental result of (a) Q from GMI and (b) required OSNR for two types of LLR calculation: ideal (dotted line) and the proposed (solid line).

transmissions. Figure 6 (b) shows required OSNR, which was calculated by loading noise at the receiver DSP to emulate OSNR decrease. The target normalized GMI was set to 0.92, which was close to 20.5% SD-FEC limit¹³. The proposed soft-demapping worked such low OSNR conditions and 4D-2A8PSK outperformed DP-Star-8QAM as the launched power increase.

Conclusions

We proposed a soft-demapping technique for MD complementary APSK signals. Combination of LLR tables and LLR updates realizes precise and flexible LLR generation with efficient hardware resources. Based on nonlinear transmission experiment with offline processing, the loss of soft-demapping is no larger than 0.15 dB and the overall improvement of 4D-2A8PSK reaches 0.5 dB in maximum Q-factor, compared to the conventional DP-Star-8QAM.

References

- [1] E. Agrell et al., J. Lightw. Technol., vol. 27, no. 22, p. 5115 (2009).
- [2] J. K. Fischer et al., J. Lightw. Technol., vol. 33, no. 7, p. 1445 (2015).
- [3] K. Kojima et al., Proc. ECOC, P.3.25 (2014).
- [4] K. Kojima et al., Proc. TIWDC, P4.5 (2015).
- [5] M. Reimer et al., Proc. OFC, M3A.4 (2015).
- [6] R. R. Müller et al., Proc. OFC, W3K.4 (2015).
- [7] S. Ishimura et al., Proc. ECOC, P.3.1 (2015).
- [8] Q. Wang et al., Proc. ACP, AS3D.2 (2015).
- [9] A. Alvarado et al., J. Lightw. Technol., vol. 33, no. 10, p. 1993 (2010).
- [10] T. Koike-Akino et al. Proc. CLEO, SW1M.3 (2015).
- [11] M. Pajovic et al., Proc. ECOC, Mo.4.3.3 (2015).
- [12] S. ten Brink et al., IEEE transactions on communications, vol. 52, no. 4, p. 670 (2004).
- [13] K. Ishii et al., Proc. ECOC, Th.3.4.2 (2015).